

The AgrD N-Terminal Leader Peptide of *Staphylococcus aureus* Has Cytolytic and Amyloidogenic Properties

Kelly Schwartz, Matthew D. Sekedat, Adnan K. Syed, Brendan O'Hara, David E. Payne, Abigail Lamb, Blaise R. Boles*

Department of Molecular, Cellular, and Developmental Biology, University of Michigan, Ann Arbor, Michigan, USA

***Staphylococcus aureus* virulence is coordinated through the Agr quorum-sensing system to produce an array of secreted molecules. One important class of secreted virulence factors is the phenol-soluble modulins (PSMs). PSMs are small-peptide toxins that have recently been characterized for their roles in infection, biofilm development, and subversion of the host immune system. In this work, we demonstrate that the signal peptide of the *S. aureus* quorum-sensing signal, AgrD, shares structural and functional similarities with the PSM family of toxins. The efficacy of this peptide (termed N-AgrD) beyond AgrD propeptide trafficking has never been described before. We observe that N-AgrD, like the PSMs, is found in the amyloid fibrils of *S. aureus* biofilms and is capable of forming and seeding amyloid fibrils *in vitro*. N-AgrD displays cytolytic and proinflammatory properties that are abrogated after fibril formation. These data suggest that the N-AgrD leader peptide affects *S. aureus* biology in a manner similar to that described previously for the PSM peptide toxins. Taken together, our findings suggest that peptide cleavage products can affect cellular function beyond their canonical roles and may represent a class of virulence factors warranting further exploration.**

Staphylococcus aureus is a common constituent of the human microflora, living commensally on the skin or in the anterior nares of approximately one-third of the population (1, 2). Despite this typically innocuous relationship, *S. aureus* can cause diseases ranging from benign skin conditions to fatal systemic infections (3–6). The severity of an *S. aureus* infection is partially attributed to toxins produced by the infecting strain, which include superantigens, alpha-toxin, leukocidins, and other small-peptide toxins, such as phenol-soluble modulins (PSMs) (7–12). PSMs are of particular interest because they perform multiple roles in pathogenesis. These short peptides compound pathogenicity by activating host receptor-mediated inflammatory responses (12–17), lysing red and white blood cells (16, 18, 19), altering biofilm development (20–23), and acting as antimicrobial agents against niche-occupying organisms in the host (24–27).

Our group has reported previously that PSMs enhance *S. aureus* biofilm structures, likely through coordinated aggregation into amyloid structures (22). Amyloid aggregates are robust fibril structures produced through the self-seeded autoaggregation of monomeric units. Mature amyloid fibrils display a characteristic cross- β -sheet structure and are strongly resistant to chemical and enzymatic degradation (28, 29). Biofilms that produced PSM fibrils were resistant to dispersal by matrix-degrading enzymes, surfactants, and mechanical disruption. Soluble PSMs dispersed biofilms, while preaggregation of PSMs into amyloid fibrils abolished this dispersal activity (22).

The *S. aureus* accessory gene regulatory (Agr) quorum-sensing system is associated with toxin production during aggressive acute infections, while in several animal models, *agr* mutants are less virulent (3, 5, 10, 30–32). Agr directly regulates the expression of all three PSM types characterized (PSM α 1–4, PSM β 1–2, and delta-toxin) (13, 33). The *agrBDCA* operon encodes the core components of the quorum-sensing system, while the divergently transcribed RNAPIII is a regulatory RNA and the primary effector of the *agr* regulon. Briefly, the Agr quorum-sensing circuit functions through the AgrCA two-component sensory complex, which detects and responds to the autoinducing peptide (AIP)

signal derived from AgrD (30, 31, 34). AgrA binds to promoters P2 and P3 to upregulate the production of the Agr machinery and the RNAPIII response element. It was thought that P2 and P3 were the exclusive targets of AgrA until it was demonstrated that AgrA binds to promoters upstream of the PSM α and PSM β operons (33). Thus, Agr and the PSMs are linked through their shared transcriptional regulation.

AgrD is translated as a propeptide composed of three parts: an N-terminal amphipathic leader, a middle region of 8 residues that is processed into the final AIP structure, and a charged C-terminal tail (see Fig. 1F) (31). The N-terminal region of AgrD is essential for directing the propeptide to the cell membrane (35), where the integral membrane endopeptidase AgrB removes the C-terminal tail, catalyzes thiolactone ring formation, and transports the AgrD AIP intermediate across the cell membrane (34, 36). Once this intermediate peptide is secreted from the cell, the SpsB signal peptidase cleaves the N-terminal peptide to release the active form of AIP, leaving the leader peptide associated with the cytoplasmic membrane (37, 38). Thus, the current model of AIP processing suggests that the N-terminal leader fragment is essential for targeting the propeptide to the cell membrane, but the fate of the peptide after AIP processing is unknown.

Here, for the first time, we provide evidence that the N-terminal amphipathic leader of the AgrD propeptide (termed N-AgrD) has multiple properties that are similar to those of the PSM pep-

Received 28 May 2014 Accepted 22 June 2014

Published ahead of print 30 June 2014

Editor: F. C. Fang

Address correspondence to Blaise R. Boles, blaise-boles@uiowa.edu.

* Present address: Blaise R. Boles, Department of Microbiology, Roy J. and Lucille A. Carver College of Medicine, University of Iowa, Iowa City, Iowa, USA.

K.S. and M.D.S. contributed equally to this article.

Copyright © 2014, American Society for Microbiology. All Rights Reserved.

doi:10.1128/IAI.02111-14

tides. N-AgrD is present in *S. aureus* amyloid fibrils during biofilm growth and is capable of autoaggregation and of seeding the amyloid polymerization of PSM peptides *in vitro*. Soluble N-AgrD is cytolytic against human cells and displays proinflammatory activity. These findings demonstrate a novel biological role for a leader peptide beyond trafficking and may provide additional context for the biological functions of staphylococcal PSMs.

MATERIALS AND METHODS

Bacterial strains and growth conditions. *S. aureus* strain LAC (methicillin-resistant *S. aureus* [MRSA] strain USA300-0114) was the wild-type strain used in this study (39). The construction of the pAgrBD plasmid has been described previously (40). Plasmid pAgrBD and an empty vector, pEPSA5, were transformed into an *S. aureus* LAC agr mutant by electroporation to create strains BB2933 (LAC agr pAgrBD) and BB2945 (LAC agr pEPSA5).

Strains were routinely grown in tryptic soy broth (TSB) incubated at 37°C with shaking at 200 rpm unless otherwise noted. The carbon-limited growth medium (CLM) for the detection of N-AgrD in culture supernatants consisted of glucose (75 mM), ammonium sulfate (7.5 mM), potassium phosphate (33 mM), and dipotassium phosphate (60 mM) supplemented with NaCl (11 mM), KCl (2 mM), Casamino Acids (0.5%; BD Biosciences), MgSO₄ (0.1 mM), and the vitamins nicotinamide (500 µg/liter), thiamine (500 µg/liter), pantothenate (500 µg/liter), and biotin (0.3 µg/liter) (40).

Biofilm experiments, amyloid fibril isolation, mass spectrometry, and microscopy. Drip flow biofilms were grown in 3.3 g/liter peptone, 2.6 g/liter NaCl, and 3.3 g/liter glucose (PNG medium) as described previously (22, 41). Amyloid fibrils were collected after 5 days of growth. Briefly, biofilms were scraped into 3 ml of potassium phosphate buffer (50 mM; pH 7) and were homogenized (TissueMiser; Fisher) to shear fibrils from the cell walls. Supernatants were clarified by repeated centrifugation at 13,000 rpm for 2 min to remove cells. The cell-free supernatant was incubated in 200 mM NaCl, and the fibrils were isolated using Millipore Amicon Ultra centrifugal filter units with a pore size of 100 kDa.

Fibril protein components were identified by liquid chromatography (LC)-tandem mass spectrometry (MS-MS) after digestion with pepsin (MS Bioworks, Ann Arbor, MI) as described previously (22). The value for the abundance measurement is the normalized spectral abundance factor (NSAF).

Transmission electron microscopy (TEM) was performed using a Philips CM12 transmission electron microscope. Samples prepared for TEM imaging were spotted onto Formvar-coated copper grids, incubated for 5 min, washed with sterile double-distilled water (ddH₂O), and negatively stained with 2% uranyl acetate for 60 s.

To detect the presence of N-AgrD in culture supernatants, cultures were grown in 100 ml CLM for 24 h at 37°C, and cells were removed by centrifugation and passage of the supernatant through a 0.22-µm filter. The supernatant was then concentrated 1,000-fold by trichloroacetic acid (TCA) precipitation and was resuspended in water. Following trypsin digestion, samples were analyzed by nano-LC-MS-MS (MS Bioworks, Ann Arbor, MI).

PSM polymerization experiments. The N-AgrD and PSMα1 peptides were synthesized by LifeTein (South Plainfield, NJ); they were assayed and found to be >90% pure by high-performance LC (HPLC). Synthetic peptides were prepared and assayed as described previously to eliminate large aggregates from lyophilization prior to the assay (22, 42). The amino acid sequence of the N-AgrD peptide was MNTLFLNLFDFITGILKNIGNIAA; the sequence of the scrambled N-AgrD peptide was LGAAFNMNLINFDFTGIFNKLITII; and the sequence of the PSMα1 peptide was MGIIAGIIVKSLIEQFTGK. Each lyophilized peptide stock was dissolved directly into hexafluoroisopropanol (HFIP) to a concentration of 0.5 mg/ml and was briefly vortexed. Peptide stocks were aliquoted into microcentrifuge tubes, and the HFIP solvent was removed by a SpeedVac system at room temperature. Dried peptide stocks were stored at -80°C.

All amyloid dye-binding assays were performed in 96-well black opaque polystyrene tissue culture (TC)-treated plates (Costar 3603; Corning). Immediately prior to the assay, dried peptide stocks were thawed and were dissolved in dimethyl sulfoxide (DMSO) to a concentration of 10 mg/ml. Freshly dissolved peptides were diluted in sterile ddH₂O containing 0.2 mM thioflavin T (ThT) and were assayed at room temperature. Fluorescence was measured every 10 min after shaking by a Tecan Infinite M200 plate reader at an excitation wavelength of 438 nm and an emission wavelength of 495 nm. ThT fluorescence during polymerization was corrected by subtracting the background intensity of an identical sample without ThT. Assays were repeated at least twice.

Congo red (CR) absorbance scans were performed on peptides that had been allowed to polymerize for 24 h in ddH₂O. Samples were incubated in 0.001% (wt/vol) CR in ddH₂O for 30 min prior to an assay on a Tecan Infinite M200 plate reader. CR scans were corrected by subtracting the background intensity of the identical sample before the addition of the dye. Assays were repeated at least twice.

CD spectroscopy. Treated peptide stocks were thawed, dissolved in HFIP to a concentration of 10 mg/ml, and incubated on ice for 20 min. Samples of 15 µM peptide were made by diluting the dissolved peptide in 500 µl sterile ddH₂O immediately prior to assay. Far-UV circular dichroism (CD) measurements were performed with a Jasco J-810 spectropolarimeter using quartz cells with a 0.1-cm path length. CD spectra between 190 and 260 nm were recorded in millidegrees and converted to molar ellipticity. The average of the results of five scans was recorded at 25°C using a 2-nm bandwidth with a scanning speed of 20 nm min⁻¹. CD scans were performed over the course of 20 h. Triplicate samples showed similar ellipticity patterns.

Hemolysis assays. The collection of blood from human subjects was approved by the University of Michigan Institutional Review Board (approval number IRB00001995). Human whole blood was washed in phosphate-buffered saline (PBS) and was diluted to a final concentration of 1:25 (vol/vol) in PBS. One hundred microliters of blood was then placed in individual wells of a flat-bottom 96-well microtiter plate (Costar 3596; Corning).

Synthetic PSMα1 and N-AgrD peptides resuspended in DMSO were added directly to the wells at the concentrations indicated in the figures, and the mixtures were incubated for 60 min at 37°C. After incubation, plates were centrifuged at 500 × g for 10 min, and an aliquot of the supernatant (100 µl) was transferred to a separate microtiter plate for the measurement of hemoglobin absorbance at 450 nm on a Tecan Infinite M200 plate reader. The assays were repeated in triplicate.

Overnight cultures of *S. aureus* containing plasmid pAgrBD or pEPSA5 were diluted 1:100 in 5 ml of TSB containing the levels of xylose indicated in Fig. 4. The cells were grown by shaking at 37°C to an optical density of 2.00 at 600 nm. The supernatants were then prepared by passage through 0.22-µm filters. Ten microliters of the supernatant was then added to 100 µl of blood, and the mixture was incubated for 60 min at 37°C. After incubation, the plates were centrifuged at 500 × g for 10 min, and an aliquot of the supernatant (optical density, 2.00) was transferred to a separate microtiter plate for the measurement of hemoglobin absorbance at 450 nm on a Tecan Infinite M200 plate reader.

Lysis of human neutrophils. Venous blood was collected from healthy human volunteers (approved by the University of Michigan Institutional Review Board; approval number IRB00001995) by using 0.2% EDTA as an anticoagulant. Neutrophils were isolated by sequential centrifugation in Ficoll Paque Plus (GE Healthcare), and hypotonic lysis of erythrocytes was carried out as described previously (12, 18). Briefly, 3.7 µM either PSMα1 or N-AgrD synthetic peptide was added to the wells of a 96-well microtiter plate containing 10⁶ neutrophils, and plates were incubated at 37°C for 2 h. The level of neutrophil lysis was determined by quantitating the release of lactate dehydrogenase (LDH) (cytotoxicity detection kit; Roche Applied Sciences). The assays were repeated in triplicate.

Measurement of IL-8 production and neutrophil chemotaxis. Neutrophil chemotaxis in the presence of 2 µM N-AgrD or PSMα1 synthetic peptide was analyzed using a QCM chemotaxis assay kit (3 µm; ECM504;

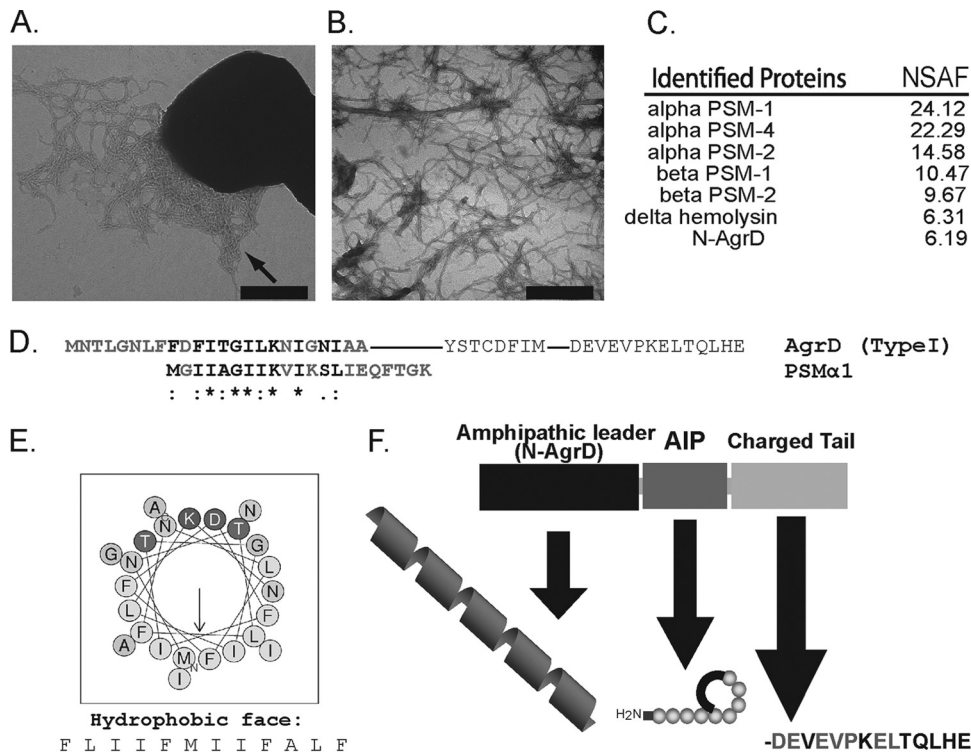


FIG 1 *S. aureus* USA300 strain LAC displays robust amyloid fibril formation. Fibrils extracted from biofilms contained high levels of phenol-soluble modulins and the N-terminal region of AgrD (N-AgrD). (A) TEM illustrating fibril formation (indicated by arrow) by *S. aureus* strain LAC after 5 days of biofilm growth. Bar, 500 nm. (B) TEM of purified fibrils subjected to MS analysis. Bar, 500 nm. (C) Peptide species identified in duplicate samples of isolated fibrils via MS analysis and their relative abundance factors within the samples (NSAF). (D) ClustalW sequence alignment illustrating the similarity of the primary structures of the N-terminal region of AgrD and PSM α 1. Residues in AgrD type I that are conserved among Agr types are shown in lightface. (E) Predicted arrangement of N-AgrD residues in an α -helical wheel showing amphipathy that is typical of PSMs (<http://heliquist.ipmc.cnrs.fr/cgi-bin/ComputParamsV2.py>). (F) Graphical illustration of AgrD propeptide domains, including the amphipathic leader sequence, the autoinducing peptide (AIP), and the C-terminal charged tail.

Millipore). Briefly, isolated human neutrophils were subjected to a brief hypotonic shock with pyrogen-free water (Sigma), washed, and suspended at 5×10^6 cells/ml in Hanks balanced salt solution (HBSS) containing 0.05% human serum albumin. Chemotaxis of neutrophils was determined by using fluorescently labeled neutrophils that migrated through a membrane fitted into an insert of a 24-well microtiter plate transwell system containing a prewetted 3- μ m-pore-size polycarbonate filter. The production of interleukin 8 (IL-8) in human neutrophils after exposure to 6 μ M N-AgrD or PSM α 1 synthetic peptide was measured by using a commercial enzyme-linked immunosorbent assay (ELISA) kit (R&D Systems) according to the manufacturer's instructions. Statistical analysis was performed using a 1-way analysis of variance (ANOVA).

RESULTS

The N-AgrD peptide is present in purified amyloid fibrils. Our previous work demonstrated that the *S. aureus* laboratory strain SH1000 produced amyloid fibrils composed primarily of PSMs (22). In the current study, we sought to investigate whether a clinical isolate produced amyloid fibrils with a composition different from that for our common lab strain. For this work, we utilized the community-associated (CA)-MRSA USA300 strain LAC, which exhibits robust Agr activity producing high levels of PSMs (12, 43). As observed by transmission electron microscopy (TEM), LAC biofilms also produced substantial quantities of extracellular fibrils that were readily isolated from cells (Fig. 1A and B). LC-MS-MS analysis of LAC biofilm fibrils confirmed that PSM species were associated with the amyloid fibrils, but we also

detected substantial quantities of the AgrD N-terminal leader peptide in our isolated fibrils (Fig. 1C and F) (22). This finding prompted our investigation to determine the relevance of the N-terminal AgrD peptide in *S. aureus* biofilms.

N-AgrD displays amyloid-like characteristics. An alignment of the N-AgrD amino acid sequence to the PSM α 1 sequence showed distinct similarity to PSM α 1 (Fig. 1D). N-AgrD has also been predicted to adopt an amphipathic α -helical structure that is similar to those of the PSMs (12, 38) (Fig. 1E). These striking primary and secondary structural similarities, combined with the observation that N-AgrD is associated with fibrils in biofilms, led us to speculate that N-AgrD may contribute to amyloid formation.

The cross- β -sheet architecture of mature amyloid fibrils can be detected using several biochemical assays, including amyloid-specific dyes and circular dichroism (28, 29, 44, 45). To test whether N-AgrD could form amyloids, we assayed the synthetic N-AgrD peptide for its ability to autoaggregate using an *in vitro* thioflavin T (ThT) fluorescence assay (46). Amyloid aggregation generally occurs in two phases: (i) a lag phase, during which monomers associate into oligomeric nuclei, and (ii) an exponential polymerization phase, during which mature amyloid fibrils are formed (a shift in ThT fluorescence occurs as ThT binds to amyloid fibrils, and fluorescence levels will increase over time as more monomers adopt the amyloid fold in solution) (46, 47). Over a 12-h time course, synthetic N-AgrD displayed an initial lag phase followed by a concentration-dependent increase in the level of ThT fluores-

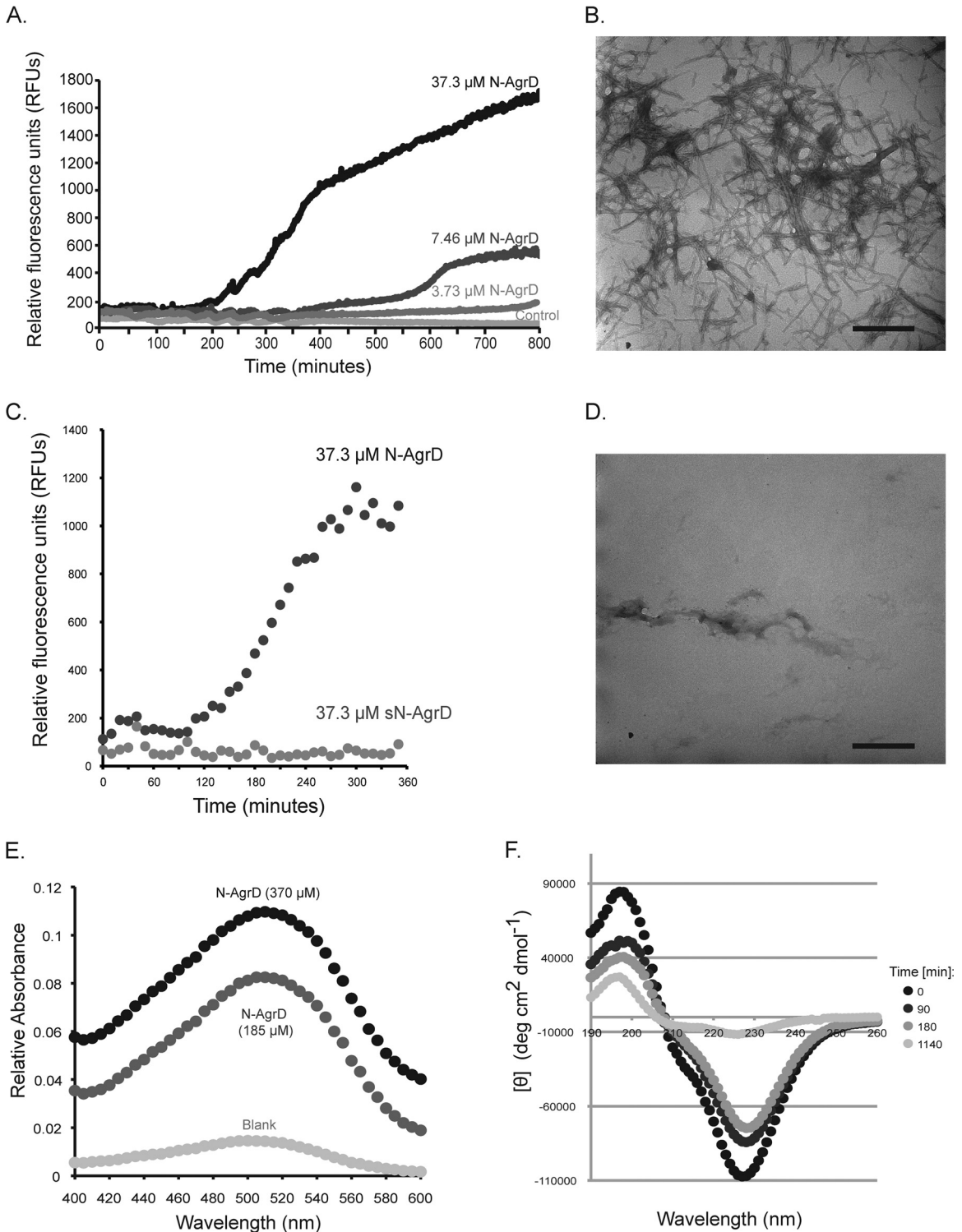


FIG 2 N-AgrD possesses amyloid-like characteristics. (A) ThT assay monitoring amyloid polymerization kinetics with the synthetic N-AgrD peptide. Normalized fluorescence intensity is shown for N-AgrD at 37.3 μM, 7.46 μM, or 3.73 μM, and for a no-peptide control, incubated with 2 mM ThT. (B) TEM of 37.3 μM N-AgrD after 24 h in solution. Bar, 500 nm. (C) A scrambled version of the N-AgrD peptide (labeled sN-AgrD) does not display amyloid ThT fluorescence, in contrast to intact N-AgrD. Peptides were assayed at a concentration of 37.3 μM. (D) TEM of 37.3 μM sN-AgrD after 24 h in solution. Bar, 500 nm. (E) CR absorbance of the N-AgrD peptide. A characteristic concentration-dependent increase in absorbance at 515 nm over that with Congo red only was seen with 370 μM or 185 μM N-AgrD. (F) CD spectroscopy of 15 μM N-AgrD peptide transitioning to a β-sheet conformation over time.

cence, indicative of amyloid assembly (Fig. 2A) (46). We verified the presence of amyloid aggregates at the end of the time course by taking TEM images of N-AgrD 24 h postinoculation. We observed fibrils with a diameter of $\sim 12 \mu\text{m}$, consistent with amyloid fibril morphology (Fig. 2B). A scrambled-peptide control (sN-AgrD) failed to display ThT fluorescence and to form fibrils, indicating that amyloid aggregation is sequence dependent (Fig. 2C and D).

To further demonstrate that the fibrils observed were amyloids, we incubated N-AgrD fibrils with another amyloid-binding dye, Congo red (CR). A characteristic “red shift” in absorbance at $\sim 515 \text{ nm}$ was observed relative to the absorbance with a buffer control, a finding indicative of the cross- β -structure of amyloid fibrils (Fig. 2E) (48). To confirm that N-AgrD was adopting a β -sheet conformation after aggregation, we used circular dichroism (CD) to assay the secondary structural changes of synthetic N-AgrD over time. As predicted, freshly dissolved peptide displayed a change in peak absorbances consistent with a transition to an increased β -sheet content over time (Fig. 2F).

Considering the sequence similarity between N-AgrD and PSM $\alpha 1$ (Fig. 1), these observations suggest a potential role for both peptides in biofilms. These biochemical and biophysical data were consistent with our hypothesis that N-AgrD is capable of forming amyloid fibrils (Fig. 2). We next aimed to investigate the biological relationship between N-AgrD and the PSM amyloids.

N-AgrD is capable of seeding PSM amyloid polymerization.

Autoaggregation of amyloid proteins is rate-limiting, but aggregation is accelerated with the addition of oligomers or preformed fibrils called “seeds” (49, 50). We asked whether polymerized N-AgrD could seed its own amyloid formation or seed the aggregation of PSM peptides (Fig. 3). The addition of 5% (wt/vol) N-AgrD fibrils (seeds) to freshly resuspended soluble N-AgrD reduced the lag phase and increased the relative ThT fluorescence intensity (Fig. 3A). The use of 5% N-AgrD seeds alone displayed negligible fluorescence throughout the duration of the experiment. A similar reduction in the lag phase was observed when N-AgrD seeds (5%) were added to freshly resuspended PSM $\alpha 1$ (Fig. 3B). These findings demonstrate that N-AgrD can seed *in vitro* amyloid formation in both N-AgrD and PSM $\alpha 1$.

Soluble N-AgrD has cytolytic activity against human cells.

PSMs are cytolytic against several host cell types, a quality that contributes to *S. aureus* infection (12, 18). Cytotoxicity is attributed to PSM peptides found as soluble species in the supernatants of liquid cultures (51, 52). Thus, we used LC-MS-MS to verify that N-AgrD is also found in culture supernatants. Indeed, we detected N-AgrD (full length [MNTLFNLFDFITGILKNIGNIAA] and two fragments [FITGILKNIGNIAA and ILKNIGNIAA]) in cell-free supernatants from *S. aureus* LAC grown in a minimal medium to late-stationary phase (data not shown).

We next tested the synthetic N-AgrD peptide for cytolytic activity (Fig. 4). Using an LDH assay as an indicator of cell lysis, we found that exposure of neutrophils to $3.7 \mu\text{M}$ N-AgrD or PSM $\alpha 1$ induced neutrophil lysis after a 90-min incubation (Fig. 4A). N-AgrD also lysed human red blood cells, resulting in 64% hemoglobin release (Fig. 4B). To determine whether amyloid formation abrogated this effect, we compared the lytic activities of N-AgrD and PSM $\alpha 1$ fibrils. Interestingly, these fibrils displayed pronounced reductions in cytotoxicity against neutrophils and red blood cells from that for freely soluble peptides (Fig. 4A and B). Taken together, these findings suggest that N-AgrD may act as a virulence factor by lysing human cells and that

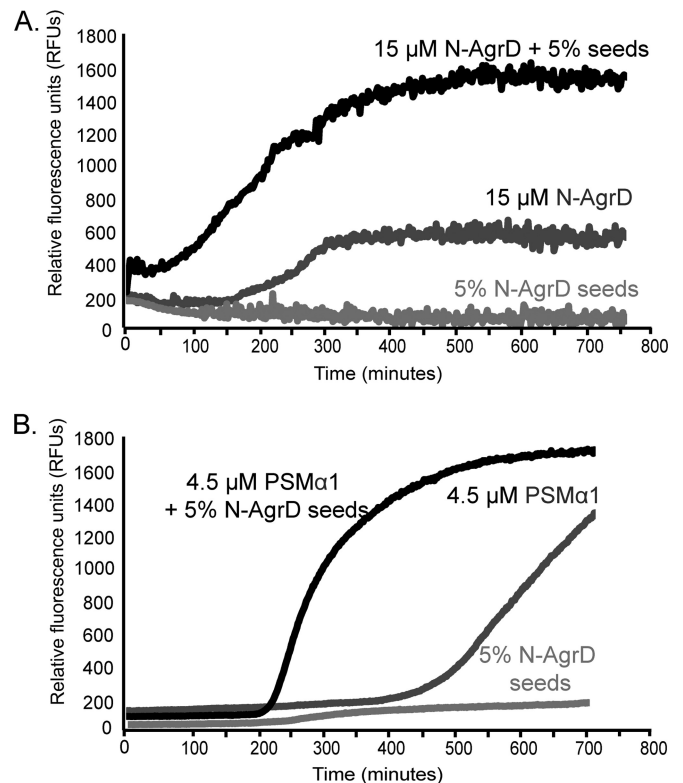


FIG 3 N-AgrD amyloid fibrils are capable of seeding amyloid formation. (A) ThT polymerization assay of $15 \mu\text{M}$ synthetic N-AgrD peptide in the presence or absence of 5% (wt/vol) sonicated N-AgrD seeds. (B) ThT polymerization assay of the PSM $\alpha 1$ peptide at $4.5 \mu\text{M}$ in the presence or absence of 5% (wt/vol) sonicated N-AgrD seeds.

this activity can be modulated by the ordered aggregation of N-AgrD and PSMs into amyloid fibrils.

To test the cytotoxicity of N-AgrD in a biological context, we overexpressed AgrD from a plasmid containing an *agrBD* construct on a xylose-inducible promoter in an *agr* mutant background (strain BB2933). *agrB* was included in this construct because it is necessary for the proper processing and secretion of the AgrD propeptide to release the N-terminal leader peptide (34, 53). *agrBD* expression resulted in increased lysis of red blood cells over that with the empty-vector control (Fig. 4C).

N-AgrD displays proinflammatory properties. PSMs can induce proinflammatory responses by neutrophils, such as neutrophil chemotaxis and IL-8 cytokine release (12–14). Since N-AgrD displayed cytolytic activity against host cells (Fig. 4), we examined the proinflammatory response to N-AgrD peptides. Human neutrophils displayed similar chemotactic responses upon exposure to soluble N-AgrD and PSM peptides, including both PSM $\alpha 1$ and delta-toxin (Fig. 5A). However, polymerization of the N-AgrD and PSM $\alpha 1$ peptides prior to the assay abrogated this neutrophil chemotactic activity (Fig. 5A).

Next, we assayed the production of the cytokine IL-8 in human neutrophils after exposure to the N-AgrD and PSM peptides. We observed robust induction of IL-8 production in response to soluble N-AgrD and PSM $\alpha 1$ that was significantly reduced in polymerized peptide samples (Fig. 5B). These findings suggest that N-AgrD promotes a proinflammatory response similar to that induced by known

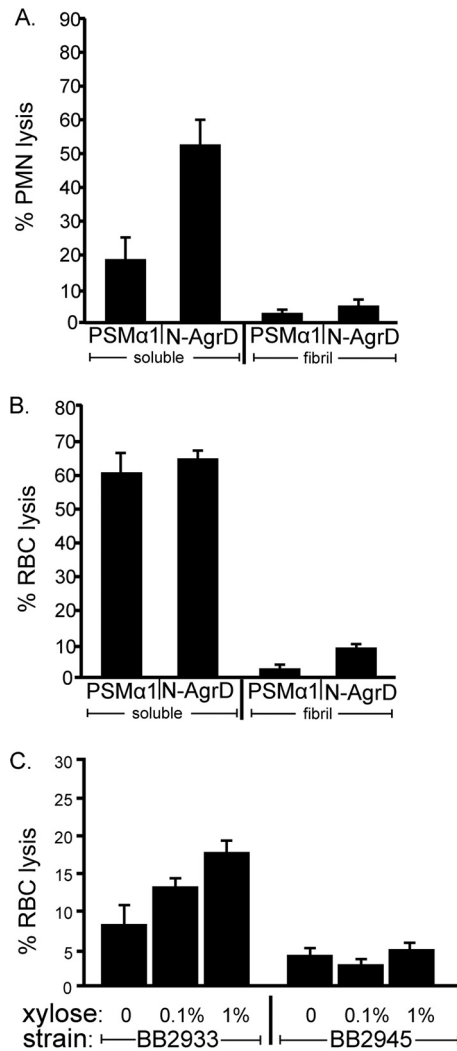


FIG 4 Soluble N-AgrD possesses cytolytic activity against human cells. (A and B) Lysis of polymorphonuclear leukocytes (PMN) (A) or red blood cells (RBC) (B) by 3.7 μ M N-AgrD or PSM α 1 after a 90-min exposure. For both assays, N-AgrD and PSM α 1 were analyzed in both the soluble and polymerized states. (C) Lysis of RBC cells after exposure to cell-free supernatants from *S. aureus* strain BB2933 (*agr* pAgrBD) or BB2945 (*agr* pEPSA5) (empty vector).

PSMs and further promote the idea that N-AgrD should be considered a PSM-like peptide in structure and activity.

DISCUSSION

PSM peptides are major determinants of *S. aureus* virulence that possess cytolytic and immune-modulating activities (12, 14, 15, 52). The high levels of PSMs produced by CA-MRSA strains such as USA300 are thought to contribute to the increased virulence of these strains (43). We demonstrated previously that under certain growth conditions, PSMs are capable of forming amyloid fibrils that protect *S. aureus* biofilms from disassembly (22). In the present study, we identify the N-terminal secretion signal peptide of AgrD as a PSM-like peptide and a supplementary component of the amyloid fibrils produced in clinically relevant CA-MRSA biofilms.

The N-AgrD peptide displays structural and functional similarity to the canonical PSM family of peptides (Fig. 1 and 2). We

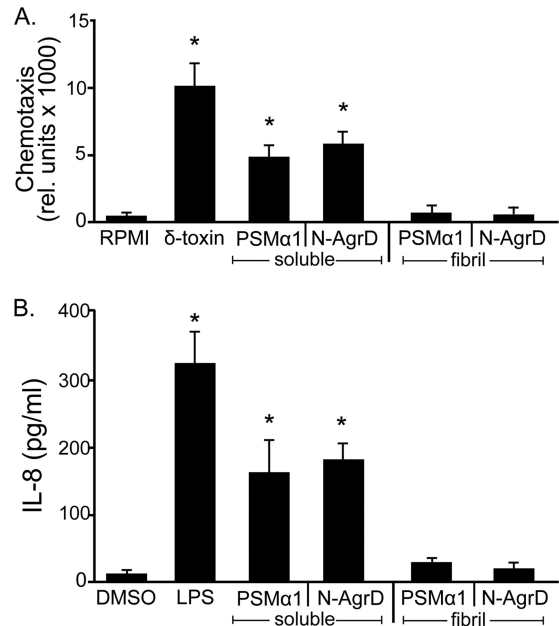


FIG 5 N-AgrD and PSM α 1 display proinflammatory activity. (A) Chemotaxis of human neutrophils. Peptides were applied at a concentration of 2 μ M. Error bars, standard errors of the means. An asterisk indicates a significant difference (P , <0.01) between samples and the RPMI medium control. (B) Secretion of IL-8 by neutrophils after treatment with N-AgrD or PSM α 1 at a concentration of 6 μ M. Lipopolysaccharide (LPS) was used at 10 ng/ml. Error bars, standard errors of the means. An asterisk indicates a significant difference (P , <0.01) between samples and the DMSO control. For both assays, N-AgrD and PSM α 1 were analyzed in both the soluble and polymerized states.

have found that N-AgrD can autoaggregate to form fibrils and that preaggregated N-AgrD can seed amyloid formation by both soluble PSM α 1 and N-AgrD (Fig. 2 and 3). N-AgrD is present in both the biofilms and the planktonic supernatants of *S. aureus* LAC bacterial cultures and also shares many biophysical characteristics with the PSMs and other amyloid proteins (Fig. 1 to 3) (22, 28). Amyloid toxicity is often attributed to the presence of reactive intermediate species (54, 55), and here we present evidence that the cytotoxic activities of N-AgrD and PSM α 1 can also be modulated through amyloid aggregation (Fig. 4). We observed high levels of cytolytic and proinflammatory activity from soluble forms of N-AgrD and PSM α 1 peptides; this activity was inhibited after aggregation (Fig. 4 and 5). Because of the striking similarities in form and function between PSM α 1 and N-AgrD, we propose that N-AgrD should be considered a new member of the PSM family.

Aside from its role in cellular trafficking, no other activity has been associated with N-AgrD. Like many signal peptides, it was considered a waste product that was simply discarded into the extracellular milieu or was associated with the cellular membrane (38, 56, 57). We provide evidence that the N-terminal signal peptide is not a waste product derived from AIP processing but instead appears to possess qualities similar to those of other peptide virulence factors known to be beneficial for the *S. aureus* life cycle.

The functions of other N-terminal leader peptides have been described in the literature. The N-terminal region of the Pantone-Valentine leukocidin (PVL) was found to promote the adhesion of *S. aureus* cells to extracellular matrix components such as heparan (58). *Enterococcus* spp. utilize a distinctive set of sex signaling pheromones that are derived from the signal peptides of lipopro-

teins (59, 60). In eukaryotic systems, signal peptides processed at the endoplasmic reticulum (ER) promote calmodulin signaling (61) and the inflammatory response (62). Many viruses, including hepatitis C virus, cytomegalovirus, and foamy viruses, utilize cleaved signal peptides to assist in cellular targeting and virus maturation (63–65). Signal peptides are being considered as novel targets for vaccine development, owing to their unique biology (66). There is even evidence that signal peptides can sequester misfolded proteins at the ER membrane to prevent toxicity (67), suggesting a potential role for N-AgrD in seeding amyloid fibril aggregation at the *S. aureus* cellular membrane.

On the basis of these published accounts, we speculate that N-AgrD, like other leader peptides previously thought only to direct protein trafficking, may also play additional roles outside of the organism after processing at the cellular membrane.

ACKNOWLEDGMENTS

We thank members of the M. Chapman laboratory for helpful discussions and suggestions.

This work was funded by an NIH grant (NIAID AI081748) to B.R.B., NIH Postdoctoral Fellowship T32HL07853-15 to M.D.S., American Heart Association Fellowship 13PRE13810001 to A.K.S., and NSF Fellowship DGE0718128 to D.E.P.

REFERENCES

- Kuehnert MJ, Kruszon-Moran D, Hill HA, McQuillan G, McAllister SK, Fosheim G, McDougal LK, Chaitram J, Jensen B, Fridkin SK, Killgore G, Tenover FC. 2006. Prevalence of *Staphylococcus aureus* nasal colonization in the United States, 2001–2002. *J. Infect. Dis.* 193:172–179. <http://dx.doi.org/10.1086/499632>.
- Wertheim H, Melles D, Vos M. 2005. The role of nasal carriage in *Staphylococcus aureus* infections. *Lancet Infect. Dis.* 5:751–762. [http://dx.doi.org/10.1016/S1473-3099\(05\)70295-4](http://dx.doi.org/10.1016/S1473-3099(05)70295-4).
- Cheung GY, Wang R, Khan BA, Sturdevant DE, Otto M. 2011. Role of the accessory gene regulator *agr* in community-associated methicillin-resistant *Staphylococcus aureus* pathogenesis. *Infect. Immun.* 79:1927–1935. <http://dx.doi.org/10.1128/IAI.00046-11>.
- Kobayashi SD, Malachowa N, Whitney AR, Braughton KR, Gardner DJ, Long D, Bubeck Wardenburg J, Schneewind O, Otto M, DeLeo FR. 2011. Comparative analysis of USA300 virulence determinants in a rabbit model of skin and soft tissue infection. *J. Infect. Dis.* 204:937–941. <http://dx.doi.org/10.1093/infdis/jir441>.
- Shaw L, Golonka E, Potempa J, Foster SJ. 2004. The role and regulation of the extracellular proteases of *Staphylococcus aureus*. *Microbiology* 150: 217–228. <http://dx.doi.org/10.1099/mic.0.26634-0>.
- Lowy FD. 1998. *Staphylococcus aureus* infections. *N. Engl. J. Med.* 339: 520–532. <http://dx.doi.org/10.1056/NEJM199808203390806>.
- Dinges MM, Orwin PM, Schlievert PM. 2000. Exotoxins of *Staphylococcus aureus*. *Clin. Microbiol. Rev.* 13:16–34. <http://dx.doi.org/10.1128/CMR.13.1.16-34.2000>.
- Peacock SJ, Moore CE, Justice A, Kantzanou M, Story L, Mackie K, O'Neill G, Day NP. 2002. Virulent combinations of adhesin and toxin genes in natural populations of *Staphylococcus aureus*. *Infect. Immun.* 70:4987–4996. <http://dx.doi.org/10.1128/IAI.70.9.4987-4996.2002>.
- Blevins JS, Beenken KE, Elasri MO, Hurlburt BK, Smeltzer MS. 2002. Strain-dependent differences in the regulatory roles of *sarA* and *agr* in *Staphylococcus aureus*. *Infect. Immun.* 70:470–480. <http://dx.doi.org/10.1128/IAI.70.2.470-480.2002>.
- Jarraud S, Mougel C, Thioulouse J. 2002. Relationships between *Staphylococcus aureus* genetic background, virulence factors, *agr* groups (alleles), and human disease. *Infect. Immun.* 70:631–641. <http://dx.doi.org/10.1128/IAI.70.2.631-641.2002>.
- Salgado-Pabon W, Breshears L, Spaulding AR, Merriman JA, Stach CS, Horswill AR, Peterson ML, Schlievert PM. 2013. Superantigens are critical for *Staphylococcus aureus* infective endocarditis, sepsis, and acute kidney injury. *mBio* 4(4):e00494–13. <http://dx.doi.org/10.1128/mBio.00494-13>.
- Wang R, Braughton KR, Kretschmer D, Bach T-HL, Queck SY, Li M, Kennedy AD, Dorward DW, Klebanoff SJ, Peschel A, DeLeo FR, Otto M. 2007. Identification of novel cytolytic peptides as key virulence determinants for community-associated MRSA. *Nat. Med.* 13:1510–1514. <http://dx.doi.org/10.1038/nm1656>.
- Kretschmer D, Nikola N, Durr M, Otto M, Peschel A. 2012. The virulence regulator Agr controls the staphylococcal capacity to activate human neutrophils via the formyl peptide receptor 2. *J. Innate Immun.* 4:201–212. <http://dx.doi.org/10.1159/000332142>.
- Kretschmer D, Gleske AK, Rautenberg M, Wang R, Koberle M, Bohn E, Schoneberg T, Rabiet MJ, Boulay F, Klebanoff SJ, van Kessel KA, van Strijp JA, Otto M, Peschel A. 2010. Human formyl peptide receptor 2 senses highly pathogenic *Staphylococcus aureus*. *Cell Host Microbe* 7:463–473. <http://dx.doi.org/10.1016/j.chom.2010.05.012>.
- Rautenberg M, Joo HS, Otto M, Peschel A. 2011. Neutrophil responses to staphylococcal pathogens and commensals via the formyl peptide receptor 2 relates to phenol-soluble modulins release and virulence. *FASEB J.* 25:1254–1263. <http://dx.doi.org/10.1096/fj.10-175208>.
- Liles WC, Thomsen AR, O'Mahony DS, Klebanoff SJ. 2001. Stimulation of human neutrophils and monocytes by staphylococcal phenol-soluble modulin. *J. Leukoc. Biol.* 70:96–102.
- Mehlin C, Headley CM, Klebanoff SJ. 1999. An inflammatory polypeptide complex from *Staphylococcus epidermidis*: isolation and characterization. *J. Exp. Med.* 189:907–918. <http://dx.doi.org/10.1084/jem.189.6.907>.
- Cheung GYC, Duong AC, Otto M. 2012. Direct and synergistic hemolysis caused by *Staphylococcus* phenol-soluble modulins: implications for diagnosis and pathogenesis. *Microbes Infect.* 14:380–386. <http://dx.doi.org/10.1016/j.micinf.2011.11.013>.
- Kantor HS, Temples B, Shaw WV. 1972. Staphylococcal delta hemolysin: purification and characterization. *Arch. Biochem. Biophys.* 151:142–156. [http://dx.doi.org/10.1016/0003-9861\(72\)90483-3](http://dx.doi.org/10.1016/0003-9861(72)90483-3).
- Wang R, Khan BA, Cheung GY, Bach TH, Jameson-Lee M, Kong KF, Queck SY, Otto M. 2011. *Staphylococcus epidermidis* surfactant peptides promote biofilm maturation and dissemination of biofilm-associated infection in mice. *J. Clin. Invest.* 121:238–248. <http://dx.doi.org/10.1172/JCI42520>.
- Kong KF, Vuong C, Otto M. 2006. *Staphylococcus* quorum sensing in biofilm formation and infection. *Int. J. Med. Microbiol.* 296:133–139. <http://dx.doi.org/10.1016/j.ijmm.2006.01.042>.
- Schwartz K, Syed AK, Stephenson RE, Rickard AH, Boles BR. 2012. Functional amyloids composed of phenol soluble modulins stabilize *Staphylococcus aureus* biofilms. *PLoS Pathog.* 8:e1002744. <http://dx.doi.org/10.1371/journal.ppat.1002744>.
- Periasamy S, Joo H-S, Duong AC, Bach T-HL, Tan VY, Chatterjee SS, Cheung GYC, Otto M. 2012. How *Staphylococcus aureus* biofilms develop their characteristic structure. *Proc. Natl. Acad. Sci. U. S. A.* 109:1281–1286. <http://dx.doi.org/10.1073/pnas.1115006109>.
- Joo H-S, Cheung GYC, Otto M. 2011. Antimicrobial activity of community-associated methicillin-resistant *Staphylococcus aureus* is caused by phenol-soluble modulin derivatives. *J. Biol. Chem.* 286:8933–8940. <http://dx.doi.org/10.1074/jbc.M111.221382>.
- Cogen AL, Yamasaki K, Muto J, Sanchez KM, Crotty Alexander L, Tanios J, Lai Y, Kim JE, Nizet V, Gallo RL. 2010. *Staphylococcus epidermidis* antimicrobial delta-toxin (phenol-soluble modulin-gamma) cooperates with host antimicrobial peptides to kill group A Streptococcus. *PLoS One* 5:e8557. <http://dx.doi.org/10.1371/journal.pone.0008557>.
- Cogen AL, Yamasaki K, Sanchez KM, Dorschner RA, Lai Y, Macleod DT, Torpey JW, Otto M, Nizet V, Kim JE, Gallo RL. 2010. Selective antimicrobial action is provided by phenol-soluble modulins derived from *Staphylococcus epidermidis*, a normal resident of the skin. *J. Invest. Dermatol.* 130:192–200. <http://dx.doi.org/10.1038/jid.2009.243>.
- Gonzalez DJ, Okumura CY, Hollands A, Kersten R, Akong-Moore K, Pence MA, Malone CL, Derieux J, Moore BS, Horswill AR, Dixon JE, Dorrestein PC, Nizet V. 2012. Novel phenol-soluble modulin derivatives in community-associated methicillin-resistant *Staphylococcus aureus* identified through imaging mass spectrometry. *J. Biol. Chem.* 287:13889–13898. <http://dx.doi.org/10.1074/jbc.M112.349860>.
- DePas WH, Chapman MR. 2012. Microbial manipulation of the amyloid fold. *Res. Microbiol.* 163:592–606. <http://dx.doi.org/10.1016/j.resmic.2012.10.009>.
- Shewmaker F, McGlinchey RP, Wickner RB. 2011. Structural insights into functional and pathological amyloid. *J. Biol. Chem.* 286:16533–16540. <http://dx.doi.org/10.1074/jbc.R111.227108>.
- Novick RP, Projan SJ, Kornblum J, Ross HF, Ji G, Kreiswirth B, Vandesch F, Moghazeh S. 1995. The *agr* P2 operon: an autocatalytic

- sensory transduction system in *Staphylococcus aureus*. *Mol. Gen. Genet.* 248:446–458. <http://dx.doi.org/10.1007/BF02191645>.
31. Ji G, Beavis RC, Novick RP. 1995. Cell density control of staphylococcal virulence mediated by an octapeptide pheromone. *Proc. Natl. Acad. Sci. U. S. A.* 92:12055–12059. <http://dx.doi.org/10.1073/pnas.92.26.12055>.
 32. Novick RP, Ross HF, Projan SJ, Kornblum J, Kreiswirth B, Moghazeh S. 1993. Synthesis of staphylococcal virulence factors is controlled by a regulatory RNA molecule. *EMBO J.* 12:3967–3975.
 33. Queck SY, Jameson-Lee M, Villaruz AE, Bach T-HL, Khan BA, Sturdevant DE, Ricklefs SM, Li M, Otto M. 2008. RNAlII-independent target gene control by the *agr* quorum-sensing system: insight into the evolution of virulence regulation in *Staphylococcus aureus*. *Mol. Cell* 32:150–158. <http://dx.doi.org/10.1016/j.molcel.2008.08.005>.
 34. Zhang L, Gray L, Novick RP, Ji G. 2002. Transmembrane topology of AgrB, the protein involved in the post-translational modification of AgrD in *Staphylococcus aureus*. *J. Biol. Chem.* 277:34736–34742. <http://dx.doi.org/10.1074/jbc.M205367200>.
 35. Zhang L. 2004. Membrane anchoring of the AgrD N-terminal amphipathic region is required for its processing to produce a quorum-sensing pheromone in *Staphylococcus aureus*. *J. Biol. Chem.* 279:19448–19456. <http://dx.doi.org/10.1074/jbc.M311349200>.
 36. Thoendel M, Horswill AR. 2009. Identification of *Staphylococcus aureus* AgrD residues required for autoinducing peptide biosynthesis. *J. Biol. Chem.* 284:21828–21838. <http://dx.doi.org/10.1074/jbc.M109.031757>.
 37. Kavanaugh JS, Thoendel M, Horswill AR. 2007. A role for type I signal peptidase in *Staphylococcus aureus* quorum sensing. *Mol. Microbiol.* 65: 780–798. <http://dx.doi.org/10.1111/j.1365-2958.2007.05830.x>.
 38. Zhang L, Lin J, Ji G. 2004. Membrane anchoring of the AgrD N-terminal amphipathic region is required for its processing to produce a quorum-sensing pheromone in *Staphylococcus aureus*. *J. Biol. Chem.* 279:19448–19456. <http://dx.doi.org/10.1074/jbc.M311349200>.
 39. Voyich JM, Braughton KR, Sturdevant DE, Whitney AR, Said-Salim B, Porcella SF, Long RD, Dorward DW, Gardner DJ, Kreiswirth BN, Musser JM, DeLeo FR. 2005. Insights into mechanisms used by *Staphylococcus aureus* to avoid destruction by human neutrophils. *J. Immunol.* 175:3907–3919. <http://dx.doi.org/10.4049/jimmunol.175.6.3907>.
 40. Thoendel M, Horswill AR. 2013. Random mutagenesis and topology analysis of the autoinducing peptide biosynthesis proteins in *Staphylococcus aureus*. *Mol. Microbiol.* 87:318–337. <http://dx.doi.org/10.1111/mmi.12100>.
 41. Schwartz K, Stephenson R, Hernandez M, Jambang N, Boles BR. 2010. The use of drip flow and rotating disk reactors for *Staphylococcus aureus* biofilm analysis. *J. Vis. Exp.* 46:2470. <http://dx.doi.org/10.3791/2470>.
 42. Wang X, Zhou Y, Ren JJ, Hammer ND, Chapman MR. 2010. Gate-keeper residues in the major curlin subunit modulate bacterial amyloid fiber biogenesis. *Proc. Natl. Acad. Sci. U. S. A.* 107:163–168. <http://dx.doi.org/10.1073/pnas.0908714107>.
 43. Li M, Diep B, Villaruz A. 2009. Evolution of virulence in epidemic community-associated methicillin-resistant *Staphylococcus aureus*. *Proc. Natl. Acad. Sci. U. S. A.* 106:5883–5888. <http://dx.doi.org/10.1073/pnas.0900743106>.
 44. Sunde M, Blake C. 1997. The structure of amyloid fibrils by electron microscopy and X-ray diffraction. *Adv. Protein Chem.* 50:123–159. [http://dx.doi.org/10.1016/S0065-3233\(08\)60320-4](http://dx.doi.org/10.1016/S0065-3233(08)60320-4).
 45. Sunde M, Serpell LC, Bartlam M, Fraser PE, Pepys MB, Blake CC. 1997. Common core structure of amyloid fibrils by synchrotron X-ray diffraction. *J. Mol. Biol.* 273:729–739. <http://dx.doi.org/10.1006/jmbi.1997.1348>.
 46. Ban T, Hamada D, Hasegawa K, Naiki H, Goto Y. 2003. Direct observation of amyloid fibril growth monitored by thioflavin T fluorescence. *J. Biol. Chem.* 278:16462–16465. <http://dx.doi.org/10.1074/jbc.C300049200>.
 47. Serio TR, Cashikar AG, Kowal AS, Sawicki GJ, Moslehi JJ, Serpell L, Arnsdorf MF, Lindquist SL. 2000. Nucleated conformational conversion and the replication of conformational information by a prion determinant. *Science* 289:1317–1321. <http://dx.doi.org/10.1126/science.289.5483.1317>.
 48. Klunk WE, Jacob RF, Mason RP. 1999. Quantifying amyloid by Congo red spectral shift assay. *Methods Enzymol.* 309:285–305. [http://dx.doi.org/10.1016/S0076-6879\(99\)09021-7](http://dx.doi.org/10.1016/S0076-6879(99)09021-7).
 49. Jarrett JT, Berger EP, Lansbury PT, Jr. 1993. The carboxy terminus of the beta amyloid protein is critical for the seeding of amyloid formation: implications for the pathogenesis of Alzheimer's disease. *Biochemistry* 32: 4693–4697. <http://dx.doi.org/10.1021/bi00069a001>.
 50. Glover JR, Kowal AS, Schirmer EC, Patino MM, Liu JJ, Lindquist S. 1997. Self-seeded fibers formed by Sup35, the protein determinant of [PSI⁺], a heritable prion-like factor of *S. cerevisiae*. *Cell* 89:811–819. [http://dx.doi.org/10.1016/S0092-8674\(00\)80264-0](http://dx.doi.org/10.1016/S0092-8674(00)80264-0).
 51. Otto M, O'Mahoney DS, Guina T, Klebanoff SJ. 2004. Activity of *Staphylococcus epidermidis* phenol-soluble modulins expressed in *Staphylococcus carnosus*. *J. Infect. Dis.* 190:748–755. <http://dx.doi.org/10.1086/422157>.
 52. Vuong C, Durr M, Carmody AB, Peschel A, Klebanoff SJ, Otto M. 2004. Regulated expression of pathogen-associated molecular pattern molecules in *Staphylococcus epidermidis*: quorum-sensing determines pro-inflammatory capacity and production of phenol-soluble modulins. *Cell. Microbiol.* 6:753–759. <http://dx.doi.org/10.1111/j.1462-5822.2004.00401.x>.
 53. Saenz HL, Augsburg V, Vuong C, Jack RW, Gotz F, Otto M. 2000. Inducible expression and cellular location of AgrB, a protein involved in the maturation of the staphylococcal quorum-sensing pheromone. *Arch. Microbiol.* 174:452–455. <http://dx.doi.org/10.1007/s002030000223>.
 54. Demuro A, Mina E, Kaye R, Milton SC, Parker I, Glabe CG. 2005. Calcium dysregulation and membrane disruption as a ubiquitous neurotoxic mechanism of soluble amyloid oligomers. *J. Biol. Chem.* 280:17294–17300. <http://dx.doi.org/10.1074/jbc.M500997200>.
 55. Kaye R, Sokolov Y, Edmonds B, McIntire TM, Milton SC, Hall JE, Glabe CG. 2004. Permeabilization of lipid bilayers is a common conformation-dependent activity of soluble amyloid oligomers in protein misfolding diseases. *J. Biol. Chem.* 279:46363–46366. <http://dx.doi.org/10.1074/jbc.C400260200>.
 56. Hegde RS, Bernstein HD. 2006. The surprising complexity of signal sequences. *Trends Biochem. Sci.* 31:563–571. <http://dx.doi.org/10.1016/j.tibs.2006.08.004>.
 57. Martoglio B, Dobberstein B. 1998. Signal sequences: more than just greasy peptides. *Trends Cell Biol.* 8:410–415. [http://dx.doi.org/10.1016/S0962-8924\(98\)01360-9](http://dx.doi.org/10.1016/S0962-8924(98)01360-9).
 58. Tristan A, Benito Y, Montserret R, Boisset S. 2009. The signal peptide of *Staphylococcus aureus* Pantone Valentine leukocidin LukS component mediates increased adhesion to heparan sulfates. *PLoS One* 4:e5042. <http://dx.doi.org/10.1371/journal.pone.0005042>.
 59. An FY, Sulavik MC, Clewell DB. 1999. Identification and characterization of a determinant (*eep*) on the *Enterococcus faecalis* chromosome that is involved in production of the peptide sex pheromone cADI. *J. Bacteriol.* 181:5915–5921.
 60. Clewell DB, An FY, Flannagan SE, Antiporta M, Dunny GM. 2000. Enterococcal sex pheromone precursors are part of signal sequences for surface lipoproteins. *Mol. Microbiol.* 35:246–247. <http://dx.doi.org/10.1046/j.1365-2958.2000.01687.x>.
 61. Martoglio B, Graf R, Dobberstein B. 1997. Signal peptide fragments of preprolactin and HIV-1 p-gp160 interact with calmodulin. *EMBO J.* 16: 6636–6645. <http://dx.doi.org/10.1093/emboj/16.22.6636>.
 62. Liu Y-S, Tsai P-W, Wang Y, Fan T-C, Hsieh C-H, Chang MD-T, Pai T-W, Huang C-F, Lan C-Y, Chang H-T. 2012. Chemoattraction of macrophages by secretory molecules derived from cells expressing the signal peptide of eosinophil cationic protein. *BMC Syst. Biol.* 6:105. <http://dx.doi.org/10.1186/1752-0509-6-105>.
 63. Prod'homme V, Tomasec P, Cunningham C, Lemberg MK, Stanton RJ, McSharry BP, Wang EC, Cuff S, Martoglio B, Davison AJ, Braud VM, Wilkinson GW. 2012. Human cytomegalovirus UL40 signal peptide regulates cell surface expression of the NK cell ligands HLA-E and gpUL18. *J. Immunol.* 188:2794–2804. <http://dx.doi.org/10.4049/jimmunol.1102068>.
 64. Lindemann D, Pietschmann T, Picard-Maureau M, Berg A, Heinkelien M, Thurow J, Knaus P, Zentgraf H, Rethwilm A. 2001. A particle-associated glycoprotein signal peptide essential for virus maturation and infectivity. *J. Virol.* 75:5762–5771. <http://dx.doi.org/10.1128/JVI.75.13.5762-5771.2001>.
 65. Okamoto K, Mori Y, Komoda Y, Okamoto T, Okochi M, Takeda M, Suzuki T, Moriishi K, Matsuura Y. 2008. Intramembrane processing by signal peptide peptidase regulates the membrane localization of hepatitis C virus core protein and viral propagation. *J. Virol.* 82:8349–8361. <http://dx.doi.org/10.1128/JVI.00306-08>.
 66. Seepersaud R, Hanniffy SB, Mayne P, Sizer P, Le Page R, Wells JM. 2005. Characterization of a novel leucine-rich repeat protein antigen from group B streptococci that elicits protective immunity. *Infect. Immun.* 73: 1671–1683. <http://dx.doi.org/10.1128/IAI.73.3.1671-1683.2005>.
 67. Schrul B, Kapp K, Sinning I, Dobberstein B. 2010. Signal peptide peptidase (SPP) assembles with substrates and misfolded membrane proteins into distinct oligomeric complexes. *Biochem. J.* 427:523–534. <http://dx.doi.org/10.1042/BJ20091005>.